THE JOURNAL OF BIOLOGICAL CHEMISTRY
Vol. 277, No. 25, Issue of June 21, pp. 22338–22344, 2002

Printed in U.S.A.

Anabaena sp. PCC 7119 Flavodoxin as Electron Carrier from Photosystem I to Ferredoxin-NADP$^+$ Reductase

ROLE OF TRP^{57} AND TYR^{94}*

Received for publication, December 21, 2001, and in revised form, April 10, 2002
Published, JBC Papers in Press, April 11, 2002, DOI 10.1074/jbc.M112258200

José L. Casaus‡, José A. Navarro§, Manuel Hervás§, Anabel Lostao‡, Miguel A. De la Rosa§, Carlos Gómez-Moreno‡, Javier Sancho‡, and Milagros Medina‡¶

From the ‡Departamento de Bioquímica y Biología Molecular y Celular, Facultad de Ciencias, Universidad de Zaragoza, Zaragoza 50009 and §Instituto de Bioquímica Vegetal y Fotosíntesis, Universidad de Sevilla-CSIC, CIC Isla de la Cartuja, Américo Vespucio s/n, Sevilla 41092, Spain

The influence of the amino acid residues sandwiching the flavin ring in flavodoxin (Fld) from the cyanobacterium *Anabaena* sp. PCC 7119 in complex formation and electron transfer (ET) with its natural partners, photosystem I (PSI) and ferredoxin-NADP$^+$ reductase (FNR), was examined in mutants of the key residues Trp^{57} and Tyr^{94}. The mutants' ability to form complexes with either FNR or PSI is similar to that of wild-type Fld. However, some of the mutants exhibit altered kinetic properties in their ET processes that can be explained in terms of altered flavin accessibility and/or thermodynamic parameters. The most noticeable alteration is produced upon replacement of Tyr^{94} by alanine. In this mutant, the processes that involve the transfer of one electron from either PSI or FNR are clearly accelerated, which might be attributable to a larger accessibility of the flavin to the reductant. However, when the opposite ET flow is analyzed with FNR, the reduced Y94A mutant transfers electrons to FNR slightly more slowly than wild type. This can be explained thermodynamically from a decrease in driving force due to the significant shift of 137 mV in the reduction potential value for the semiquinone/hydroquinone couple (E_1) of Y94A, relative to wild type (Lostao, A., Gómez-Moreno, C., Mayhew, S. G., and Sancho, J. (1997) *Biochemistry* 36, 14334–14344). The behavior of the rest of the mutants can be explained in the same way. Overall, our data indicate that Trp^{57} and Tyr^{94} do not play any active role in flavodoxin redox reactions providing a path for the electrons but are rather involved in setting an appropriate structural and electronic environment that modulates *in vivo* ET from PSI to FNR while providing a tight FMN binding.

Flavodoxins are small α/β flavoproteins involved in ET[1] reactions in microorganisms and certain algae. They can be synthesized constitutively or induced by a lack of iron in the culture medium (1, 2). The principal feature of flavodoxins is that they contain a noncovalently bound low potential flavin cofactor (FMN) that confers redox properties to the protein. The binding of FMN to flavodoxin considerably increases the stability of the cofactor semiquinone state by altering its reduction potentials. Typically, the midpoint potential for the quinone/semiquinone couple, E_2, is increased, whereas that of the semiquinone/hydroquinone couple, E_1, is decreased. This allows flavodoxin to behave as a one-electron transfer center that cycles *in vivo* between the semiquinone and the fully reduced forms (1, 3).

The three-dimensional structures of several flavodoxins are known (4–10). In most flavodoxins, the isoalloxazine ring (the redox-active moiety of FMN) is stacked between two aromatic residues. One of them is a widely conserved tyrosine that makes extensive contacts with the isoalloxazine, whereas the other aromatic residue is usually a tryptophan that interacts mainly with the two methyl groups of the isoalloxazine (11). The proximity of the two aromatic residues to the flavin ring makes them interesting candidates to play a role in modulating the reduction potentials of flavodoxin and, therefore, modulating the protein's ability to play specific functions in the electron transfer chains where it is involved. The influence of these aromatic residues on FMN binding, flavodoxin reduction potentials, and electron spin density distribution of the semiquinone state has been studied by site-directed mutagenesis using flavodoxins from different sources (11–14), and structures for some of these mutants are available (15). However, to the best of our knowledge, the influence of these aromatic residues on flavodoxin ET reactions has not been analyzed. In *Anabaena* Fld, the functionality of site-directed mutants with removal of surface negative side chains has been reported, not only with its physiological partners (PSI and FNR) but also with other ET proteins (16, 17). The introduced mutations exerted only little effects on the reactions with FNR and PSI, whereas they showed larger effects on the nonphysiological reactions with cytochrome *c* and cytochrome P450.

In *Anabaena* sp. PCC 7119 Fld, the flavin-sandwiching residues are Trp^{57} and Tyr^{94} (the only side chains in contact with the flavin ring) (9). Previous characterization of several *Anabaena* sp. PCC 7119 Fld mutants at positions 57 and 94 has

* This work was supported by Comisión Interministerial de Ciencia y Tecnología Grant BIO2000-1259 (to C. G.-M.), CONSI+D, Diputación General de Aragón, Grant P006/2000 (to M. M.), Comisión Interministerial de Ciencia y Tecnología Grant BQU2001-2520 (to M. M.), Dirección General de Estudios Superiores Grant PB97-1027 and Grant BMC 2001-2522 (to J. S.), Dirección General de Investigación Grant BMC2000-0444 (to M. A. R.), European Union Networks ERB-FMRXCT98-0218 and HPRN-CT1999-00095 (to M. A. R.), and Junta de Andalucía Plan Andaluz de Investigación Grant CVI-0198 (to M. A. R.). The costs of publication of this article were defrayed in part by the payment of page charges. This article must therefore be hereby marked "*advertisement*" in accordance with 18 U.S.C. Section 1734 solely to indicate this fact.

¶ To whom correspondence should be addressed: Dept. de Bioquímica y Biología Molecular y Celular, Facultad de Ciencias, Universidad de Zaragoza, Zaragoza 50009, Spain. Tel.: 34-976-762476; Fax: 34-976-762123; E-mail: mmedina@posta.unizar.es.

[1] The abbreviations used are: ET, electron transfer; dRf, 5-deazariboflavin; dRfH$^{\cdot}$, semiquinone form of dRf; Fld, flavodoxin; Fld$_{ox}$, Fld in the oxidized state; Fld$_{rd}$, Fld in the reduced state; Fld$_{sq}$, Fld in the semiquinone state; FNR, ferredoxin-NADP$^+$ reductase; FNR$_{ox}$, FNR in the oxidized state; FNR$_{rd}$, FNR in the reduced state; FNR$_{sq}$, FNR in the semiquinone state; PSI, photosystem I; WT, wild-type; Tricine, *N*-[2-hydroxy-1,1-bis(hydroxymethyl)ethyl]glycine.

shown that these aromatic residues, in particular Tyr^{94}, influence the cofactor reduction potentials and its absorption spectrum. In addition, measurement of the apoflavodoxin-FMN complex binding energies showed that both Tyr^{94} and Trp^{57} strengthen the interaction of apoflavodoxin with FMN in the different redox states and are responsible for setting the characteristic reduction potentials exhibited by this protein (11). In contrast, it has been shown that replacement of Tyr^{94} and Trp^{57} only very slightly influences the electron spin density distribution in the flavodoxin semiquinone state (14). In the present study, we report the functional characterization of *Anabaena* sp. PCC 7119 Fld mutants obtained by replacement of Trp^{57} and Tyr^{94} by other aromatic residues as well as by alanine and leucine (11). Complex formation and ET between PSI and Fld and between Fld and FNR have been studied for the WT and mutated forms of Fld in order to analyze the involvement of Tyr^{94} and Trp^{57} in these processes. So far, none of the three-dimensional structures of the mutants here characterized is available. However, recently, the structures of two Fld mutants from *Desulfovibrio vulgaris* at the equivalent position to Tyr^{94} from *Anabaena* Fld, Y98H and Y98W, have been reported (15). Since precise main-chain and side-chain superposition is observed between the structures of WT Flds from both species, specially around the flavin ring, the functional behavior of the *Anabaena* mutants is discussed based on the structural features observed for these two *D. vulgaris* mutant structures.

EXPERIMENTAL PROCEDURES

Biological Material—Fld mutants from *Anabaena* sp. PCC 7119 were prepared by oligonucleotide-directed mutation of the Fld gene, overproduced in *Escherichia coli*, and purified as previously described (10, 11). *Anabaena* sp. PCC 7119 WT FNR was purified from *E. coli* isopropyl-β-D-thiogalactoside-induced cultures that had been previously transformed with the *ptrc99a* vector containing the FNR gene from *Anabaena* sp. PCC 7119, as previously described (18). UV-visible spectra and SDS-PAGE electrophoresis were used as purity criteria. PSI particles from *Anabaena* sp. PCC 7119 were obtained by β-dodecyl maltoside solubilization as described by Rögner *et al.* (19) and modified by Hervás *et al.* (20). The P700 content in PSI samples was calculated from the photoinduced absorbance changes at 820 nm using the absorption coefficient of 6.5 mM^{-1} cm^{-1} determined by Mathis and Sétif (21). Chlorophyll concentration was determined according to Arnon (22). The chlorophyll/P700 ratio of the resulting PSI preparations was 140:1. The same batches of PSI and flavoproteins were used throughout this study.

Spectral Analysis—UV-visible spectra were recorded on a KONTRON Uvikon 942 spectrophotometer. Dissociation constants, binding energies, and changes in extinction coefficients for the complexes between WT FNR_{ox} and the different Fld_{ox} variants were obtained by differential spectroscopy as previously described (18). The experiments were performed on solutions containing ~20 μM FNR in 4 mM potassium phosphate, 1 mM EDTA buffer (pH 7.0) at 25 ± 1 °C, to which aliquots of the different Fld forms were added. Dissociation constants and differential extinction coefficients for the complexes were obtained by fitting the experimental data to the theoretical equation for a 1:1 stoichiometric complex by means of nonlinear regressions.

Steady-state Enzymatic Assays—The NADPH-dependent cytochrome *c* reductase activity of FNR was determined using the different Fld mutants as the electron carrier from FNR to cytochrome *c* (18, 23). To calculate the FNR K_m values for each Fld variant, the standard reaction mixtures contained 50 μM NADPH, 2.5 nM FNR, 0.75 mM cytochrome *c* (Sigma), and different concentrations of the corresponding Fld mutant. All measurements were carried out at 25 ± 1 °C in 50 mM Tris/HCl, pH 8.0.

Stopped-flow Kinetic Measurements—ET reactions between FNR and Fld were studied by stopped flow under anaerobic conditions in an Applied Photophysics SX17.MV spectrophotometer interfaced with an Acorn 5000 computer, using the SX.18MV software of Applied Photophysics as previously described (18). The apparent observed rate constants (k_{app}) were calculated by fitting the experimental data to mono- or biexponential kinetics. Samples were made anaerobic (in specially designed tonometers, which fitted the stopped-flow apparatus) by successive evacuation and O_2-free argon flushing. Reduced samples of FNR and Fld for stopped flow were prepared by photoreduction with 5-dRf as described (18). All reactions were carried out in 4 mM potassium phosphate, 1 mM EDTA, pH 7.0, at 13 ± 1 °C and followed at 600 nm, the wavelength at which semiquinone formation of both flavoproteins can be followed. FNR and Fld were mixed at 1:1 ratios with final protein concentrations ranging from 7 to 9 μM. Each kinetic trace was the average of 4–10 independent measurements. Errors in the determination of the apparent observed rate constant values (k_{app}) were of ±10%.

Laser Flash Absorption Spectroscopy—The laser flash system was based on a PTI PL-2300 nitrogen laser (emission wavelength, 337 nm; flash duration, 0.6 ns; output energy, 1.4 mJ). The laser beam was attenuated by 80% with calibrated neutral density filters. Kinetic traces of flash-induced absorbance changes at 580 nm were recorded using a Nicolet 450 digital oscilloscope. The analysis light source was a 100-watt tungsten-halogen lamp, which passed through an Oriel monochromator (model 77250, bandwidth 10 nm). The detection photomultiplier (Hamamatsu R928) was protected from actinic light by a second monochromator (Jobin-Yvon; model H-20, bandwidth 1 nm). The wavelength of 580 nm was chosen to monitor Fld semiquinone formation with the lowest possible contribution of PSI to the absorbance change. All of the experiments were carried out in a 1-cm path length cuvette at 22 ± 1 °C. Unless otherwise stated, the standard reaction mixture contained, in a final volume of 1 ml, 20 mM Tricine/KOH, pH 7.5, 0.03% β-dodecyl maltoside, an amount of PSI-enriched particles equivalent to 35 μg of chlorophyll ml^{-1}, 0.1 μM phenazine methosulfate, 2 mM $MgCl_2$, 2 mM sodium ascorbate, and Fld at the indicated concentration. Ascorbate and phenazine methosulfate addition ensures that PSI is totally rereduced between flashes. Each kinetic trace was the average of 40–50 independent measurements with 30-s spacing between flashes. Samples were protected from actinic light between flashes by an electronic shutter synchronized with the laser trigger. For most experiments, the estimated error in the observed rate constants was less than 20%, based on reproducibility and signal-to-noise ratios. Data collection was as previously described (24). Exponential analyses of the oscilloscope traces were performed using the Marquardt method with the software devised by P. Sétif (Saclay, France). Kinetic analyses were carried out according to the two-step reaction mechanism previously proposed (24, 25). Errors in the estimated values of constants for complex association (K_a) and electron transfer (k_{et}) were of ±15 and ±5%, respectively. The putative protonation rate constant of Fld semiquinone (k_{prot}) after reduction by $dRfH^{\cdot}$ was determined by following the absorbance decrease and increase at 465 and 580 nm, respectively (26).

TABLE I

Midpoint reduction potentials of the different Flds (data from Ref. 11) and steady-state kinetics parameters of WT FNR in the NADPH-dependent cytochrome c reductase activity using WT and mutant Flds as electron carrier

Fld	Reduction Potentials[a]		Steady-state kinetic parameters		
	E_2	E_1	k_{cat}	K_m	k_{cat}/K_m
	mV		s^{-1}	*mM*	mM^{-1} s^{-1}
WT	−212	−436	43 ± 1	42 ± 1	1.0 ± 0.1
Y94A	−203	−299	222 ± 7	20 ± 5	12 ± 3
Y94F	−186	−436	24 ± 4	48 ± 8	0.5 ± 0.2
Y94W	−182	−462	<5[b]	ND[b]	ND
W57F	−152	−432	37 ± 3	39 ± 4	1.0 ± 0.1
W57L	−212	−407	20 ± 3	21 ± 5	1.0 ± 0.5
W57A	−173	−417	18 ± 2	12 ± 4	1.5 ± 0.9
W57Y	−139	−447	36 ± 4	27 ± 6	1.4 ± 0.5

[a] Data from Ref. 11.

[b] Only an estimation of k_{cat} was possible due to the very low amount of reaction observed, which was independent of Fld concentration.

RESULTS

Steady-state Kinetics Analysis of the Different Fld Mutants—The catalytic properties of FNR for the flavodoxin-mediated NADPH-dependent cytochrome *c* reductase assay have been determined under steady-state conditions using WT and mutated flavodoxins. This activity involves, in addition to FNR reduction by the pyridine nucleotide, the interaction and ET between FNR and Fld and the final reduction of cytochrome *c* by the semiquinone form of Fld (18). As shown in Table I, most Fld mutants yield k_{cat} values within a factor of 2 of WT, but significant differences are observed when Y94A or Y94W are used. The value for k_{cat} with Y94A increases 5-fold relative to

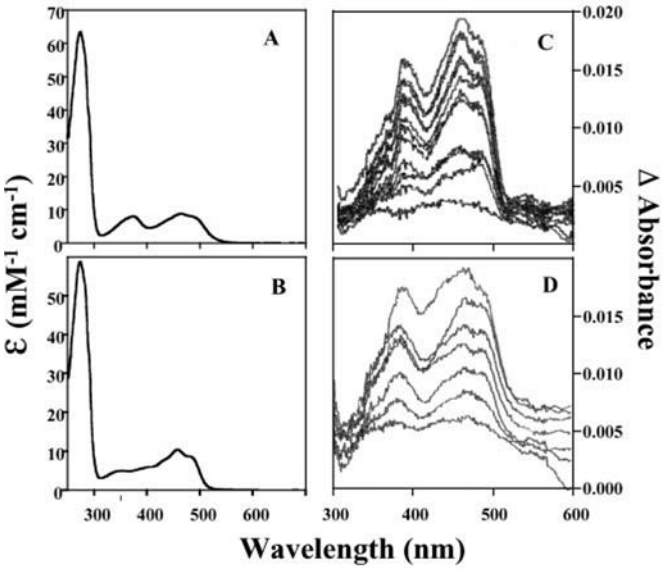

FIG. 1. **Spectroscopic characterization of the complexes formed between selected Fld_{ox} forms and FNR_{ox}.** *A*, absorption spectra of WT Fld_{ox}. *B*, absorption spectra of Y94F Fld_{ox}. *C*, difference absorption spectra obtained during the titration of WT FNR_{ox} (17.8 μM) with WT Fld_{ox}. *D*, difference absorption spectra obtained during the titration of WT FNR_{ox} (16.4 μM) with Y94F Fld_{ox}.

WT, whereas Y94W displays little activity and an estimated k_{cat} value at least 7-fold lower than WT. Unlike WT Fld, which is much less efficient than ferredoxin in this assay, the Y94A Fld mutant (k_{cat} = 222 ± 7 s^{-1}) is an ET mediator as efficient as the iron-sulfur protein (k_{cat} = 200 ± 10 s^{-1} (18)).

FNR K_m values for most Fld mutants were within a factor of 2 of WT (Table I). Only W57A showed a significant decrease in K_m (4-fold). These data suggest that the affinity of the FNR·Fld complex is hardly modified by the mutations. The K_m for Y94W could not be determined due to the lack of activity observed in the assay.

When the catalytic efficiency (k_{cat}/K_m) of FNR was determined using different Fld variants in the cytochrome *c* assay, it turned out that most Flds lead to an FNR catalytic efficiency similar to that of WT. In contrast, Y94A appeared to be 1 order of magnitude more efficient than WT, and Y94W was almost nonreactive. The higher efficiency of Y94A reflects the much faster ET process, whereas the low efficiency of Y94W could be due either to a much slower ET process or to the formation of a nonproductive interaction between Fld and either FNR or cytochrome *c*.

Interaction of Fld_{ox} Variants with FNR_{ox}—To investigate the effect of the Fld mutations at positions 57 and 94 on its interaction with FNR, difference absorption spectroscopy was used to directly evaluate the dissociation constants of the oxidized complexes (Fig. 1). The differential spectrum of the WT Fld_{ox}·FNR_{ox} complex that has been proposed to arise from alteration of the flavin environments upon Fld·FNR association shows absorption maxima around 390 and 465 nm (18). Similar spectral perturbations were detected for all of the Fld mutants studied here upon mixing with FNR_{ox}. It is worth noting the similar shape of the differential spectra obtained with the different Fld mutants, with bands around 390 and 464–480 nm with the same relative intensity as for the WT Fld complex (Fig. 1) despite the fact that some Fld mutants (*i.e.* Y94W and, especially, Y94F) present unusual flavin absorption spectra (Fig. 1*D*) (11). This suggests that the Fld_{ox}·FNR_{ox} difference spectrum is mainly due to alteration of the FAD absorption in FNR and indicates that the orientation of the two proteins in the complex is not altered by the mutations here studied.

TABLE II
Dissociation constants, differential extinction coefficients, and free energies for complex formation of oxidized WT FNR with oxidized WT and mutated Flds

Fld	K_d	$\Delta\varepsilon_{465\ nm}$	ΔG^0
	mM	$mM^{-1}\ cm^{-1}$	*Kcal* mol^{-1}
WT	3.6 ± 1.0	1.5 ± 0.2	7.4 ± 0.1
Y94A	2.3 ± 0.5	2.6 ± 0.4	7.7 ± 0.3
Y94W	6.0 ± 1.5	3.2 ± 0.6	7.2 ± 0.3
Y94F	1.0 ± 0.5	1.6 ± 0.5	8.2 ± 0.3
W57F	4.0 ± 0.8	1.0 ± 0.1	7.4 ± 0.2
W57L	2.8 ± 0.5	1.2 ± 0.1	7.5 ± 0.1
W57A	4.5 ± 1.0	1.0 ± 0.3	7.4 ± 0.6
W57Y	2.2 ± 0.8	2.0 ± 0.6	7.7 ± 0.3

Accordingly, all Fld_{ox} mutants showed similar K_d values to the WT complex (Table II). Moreover, the $\Delta\epsilon$ values for transition band I are not far from the value obtained for the WT Fld complex, with the maximal changes observed for Y94A and Y94W, whose $\Delta\epsilon$ value are ~2-fold larger. This incremented $\Delta\epsilon$ could be related with the alterations described in the absorption spectra of these mutants (11). Taken together, these data indicate that Trp^{57} and Tyr^{94} exert little influence on the orientation and strength of the FNR_{ox}·Fld_{ox} association.

Fast Kinetic Analysis of the Interaction and ET Process between FNR and Fld Mutants as Studied by Stopped Flow—To further investigate the role of Fld Trp^{57} and Tyr^{94} in association and ET to FNR, anaerobic stopped-flow kinetic experiments were carried out. The reactions between the different redox states of Fld and FNR were analyzed by following semiquinone formation at 600 nm by mixing equimolecular amounts of both proteins, each in a different redox state, either oxidized or reduced. When FNR_{ox} was mixed with Fld_{rd}, an increase in absorbance at 600 nm, previously ascribed to formation of both semiquinones (18), was detected for WT Fld (not shown) and all of the mutants (Fig. 2). For WT, Y94F, and W57L Fld, most of the reaction takes place within the instrumental dead time (~3 ms) (Table III), whereas slower processes are observed for the rest of the mutants. When the reaction of Y94A was analyzed, the kinetic traces were best fitted by a two-exponential equation, with k_{app} values of 356 and 64 s^{-1} (Fig. 2*A*). A similar behavior was observed for W57A, although in this case the first process takes place mainly within the instrumental dead time (Fig. 2*B*, Table III). In both cases, the initial process is consistent with the formation of the two semiquinones (Reaction 1), followed by reduction of FNR_{sq} to the fully reduced state by Fld_{rd}, which is still in the mixture (Reaction 2) (18).

$$FNR_{ox} + Fld_{rd} \{\overset{K_d}{\rightleftharpoons} [FNR_{ox}\cdot\cdot\cdot Fld_{rd}] \overset{k_{et}}{\longrightarrow}\} FNR_{sq} + Fld_{sq} \qquad k_{app1}$$

$$Fld_{rd} + FNR_{sq} \{\overset{K_d'}{\rightleftharpoons} [FNR_{sq}\cdot\cdot\cdot Fld_{rd}] \overset{k_{et}'}{\longrightarrow}\} Fld_{sq} + FNR_{rd} \qquad k_{app2}$$

REACTIONS 1 AND 2

More noticeable are the kinetics of Y94W, W57F, and W57Y (Fig. 2*B*). In these mutants, a lag phase with no absorbance changes is observed, both at 600 nm (Fig. 2*B*) and at 460 nm (not shown). This indicates that the accumulation of an obligatory intermediate species takes place prior to ET. Moreover, when the intermediate accumulates and the reaction starts, processes much slower than that with WT Fld take place (Table III), and they appear to occur only to a minor extent, as de-

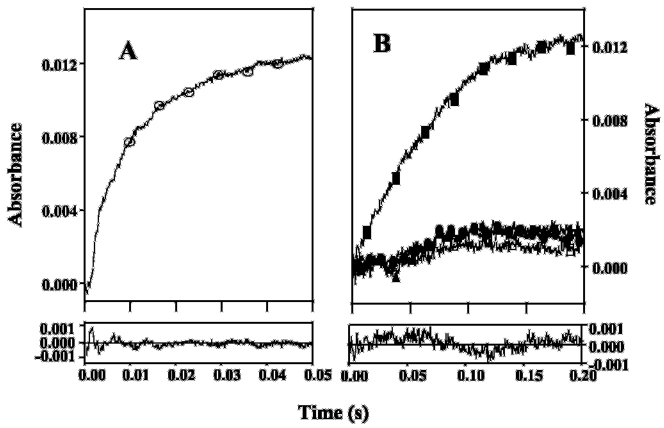

FIG. 2. **Time course of the anaerobic reactions between WT FNR_{ox} with different Fld_{rd} mutants as measured by stopped flow.** The monitoring wavelength was 600 nm. Final concentrations are given in *parentheses*. *A*, reaction of WT FNR_{ox} (8.5 μM) with Y94A Fld_{rd} (8.5 μM) (residual for this fitting is shown at the *bottom*). *B*, reaction of WT FNR_{ox} (7.5 μM) with W57A Fld_{rd} (7.5 μM) (*filled squares*; residual for this fitting is shown at the *bottom*); WT FNR_{ox} (8.1 μM) with W57F Fld_{rd} (8.6 μM) (*filled triangles*); WT FNR_{ox} (8.2 μM) with W57Y Fld_{rd} (8.6 μM) (*filled diamonds*) and WT FNR_{ox} (8.4 μM) with Y94W Fld_{rd} (8.6 μM) (*filled circles*).

TABLE III
Kinetic parameters for the reactions of WT FNR with WT and mutated Flds as studied by stopped flow

Samples were mixed in the stopped-flow instrument at equimolecular concentrations (~8 μM final concentration) and at the indicated redox states, T^a = 13 ± 1 °C. Reactions were followed at 600 nm.

Fld	$FNR_{ox} + Fld_{rd}$		$FNR_{rd} + Fld_{ox}$	
	k_{app1}	k_{app2}	k_{app1}	k_{app2}
	s^{-1}		s^{-1}	
WT	>600[a]		1.8	0.8
Y94A	356	64	400.0	
Y94F	>600[a]		1.8	1.1
Y94W	54[b]		0.5	0.06
W57F	35[b]		12.0	1.9
W57L	>600[a]		3.8	2.3
W57A	>600[a]	146	14.0	0.5
W57Y	34[b]		5.1	0.8

[a] Most of the reaction occurred within the instrumental dead time.
[b] A lag phase is observed at 600 nm until 30–50 ms; the k_{app} was estimated after this phase.

duced from their low amplitudes (Fig. 2*B*). The initial lag phase could reflect a reorganization of the initial complex, required to achieve an orientation competent for efficient ET.

The reverse reaction has also been investigated. Previous stopped-flow studies on the reaction of FNR_{rd} with WT Fld_{ox} indicated that this reaction was a relatively slow process for which two phases were detected (18). These were assigned to the following processes.

$$Fld_{ox} + FNR_{rd} \{\overset{K_d}{\rightleftharpoons} [FNR_{rd}\cdots Fld_{ox}] \overset{k_{et}}{\longrightarrow}\} Fld_{sq} + FNR_{sq} \quad (k_{app1})$$

$$Fld_{ox} + FNR_{sq} \{\overset{K_d'}{\rightleftharpoons} [FNR_{sq}\cdots Fld_{ox}] \overset{k_{et}'}{\longrightarrow}\} Fld_{sq} + FNR_{ox} \quad (k_{app2})$$

REACTIONS 3 AND 4

When this reaction was performed using different Fld mutants, a biphasic behavior, with two phases of similar amplitude, was detected for most mutants (Fig. 3*A*), as in the WT Fld

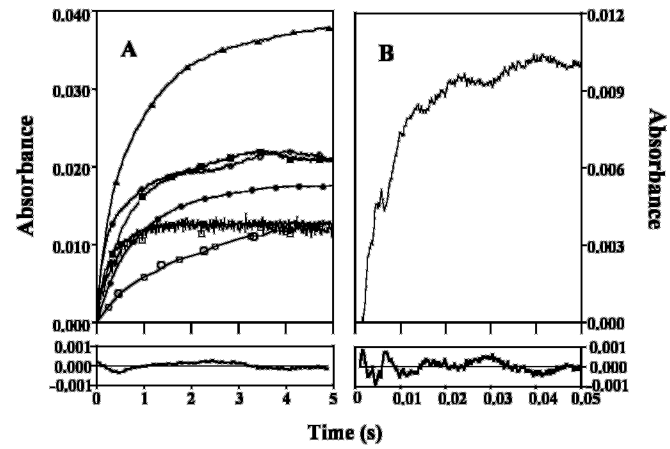

FIG. 3. **Time course of the anaerobic reactions between WT FNR_{rd} with different Fld_{ox} mutants as measured by stopped flow.** The monitoring wavelength was 600 nm. Final concentrations are given in *parentheses*. *A*, reaction of WT FNR_{rd} (8 μM) with WT Fld_{ox} (8.5 μM) (*filled diamonds*); WT FNR_{rd} (8.7 μM) with W57A Fld_{ox} (8.2 μM) (*open diamonds*); WT FNR_{rd} (8.7 μM) with W57F Fld_{ox} (9 μM) (*filled circles*); WT FNR_{rd} (10 μM) with W57Y Fld_{ox} (9 μM) (*filled triangles*; residual for this fitting is shown at the *bottom*); WT FNR_{rd} (8.1 μM) with W57L Fld_{ox} (8 μM) (*open squares*); WT FNR_{rd} (7.8 μM) with Y94F Fld_{ox} (8 μM) (*filled squares*) and WT FNR_{rd} (8.5 μM) with Y94W Fld_{ox} (8.5 μM) (*open circles*). *B*, reaction of WT FNR_{rd} (7.5 μM) with Y94A Fld_{ox} (7.5 μM) (residual for this fitting is shown at the *bottom*).

reaction. Thus, for Y94F, Y94W, and W57L Fld, the reaction takes place with k_{app} values within a factor of 2 of those with WT Fld (Table III), although the k_{app} for the second reaction of Y94W is significantly slower. Replacement of Trp^{57} either by phenylalanine, alanine or tyrosine produced larger k_{app} values (up to a factor of 7 for W57A in the first process; Table III). In all of these cases, the tryptophan side-chain has been replaced by shorter residues. Finally, we notice the effect produced by replacement of Tyr^{94} by alanine. Its reduction by FNR_{rd} fits to a monoexponential process with a k_{app} value 175-fold higher than that observed for WT Fld (Fig. 3*B*, Table III), indicating that removal of the aromatic side chain at position 94 produces an important effect in the ET mechanism from FNR to Fld. The monoexponential behavior observed for this mutant might be due either to an almost full consumption of FNR_{rd} by the first process (Reaction 3) or to a change in the mechanism of ET from the reduced FAD to the Fld FMN.

Kinetic Analysis of the Laser Flash Fast Reduction of Fld Variants by PSI—Previous studies have shown that the reduction of *Anabaena* Fld_{ox} to the semiquinone state by spinach PSI particles can be followed using laser-flash absorption spectroscopy (27). The study of the semiquinone formation constitutes a useful reaction model to analyze the interaction forces and electron transfer parameters involved in the reduction of Fld by PSI (16, 27, 28). In the present work, we have analyzed the reactivity of *Anabaena* Fld toward PSI from the same species. Reduction of Fld mutants by PSI particles followed monoexponential kinetics for WT and all of the mutants (even at high flavoprotein concentration). Fig. 4 reproduces the oscilloscope traces obtained for Y94A, W57Y, and WT Flds and shows that the reaction is much slower with W57Y than with Y94A or WT. The observed pseudo-first order rate constants (k_{obs}) of WT and mutant Fld reduction by PSI depend nonlinearly on the concentration of flavoprotein and show a saturation profile (Fig. 5). This suggests that a bimolecular transient (PSI·Fld) complex is formed prior to ET, according to the following minimal two-step reaction mechanism, as described previously in other PSI/Fld systems (16, 27, 28).

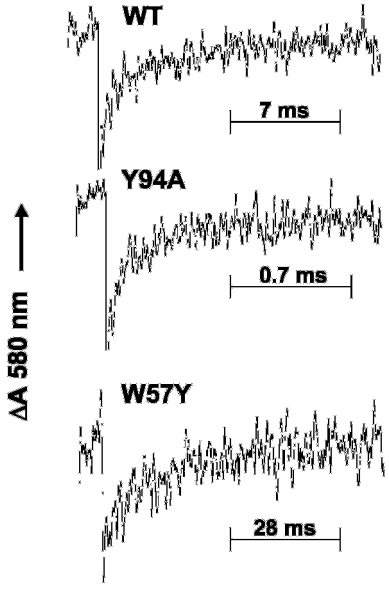

FIG. 4. **Kinetic traces showing WT and mutant Flds reduction by *Anabaena* PSI.** Flavoprotein concentration was 20 μM, and the pH value was 7.5. All kinetic traces were well fitted to single exponential curves. Other conditions were as described under "Experimental Procedures."

$$PSI_{rd} + Fld_{ox} \overset{K_a}{\rightleftharpoons} [PSI_{rd}\cdot\cdot\cdot Fld_{ox}] \overset{k_{et}}{\longrightarrow} PSI_{ox} + Fld_{sq}$$

REACTION 5

in which the electron transfer first-order rate constant (k_{et}) can experimentally be inferred from the limiting k_{obs} at infinite Fld concentration, whereas K_a is the equilibrium constant of the complex. Minimal values for K_a and k_{et}, which can be estimated from data like that in Fig. 5 using the formalism developed by Meyer *et al.* (25), are shown in Table IV for WT and mutant Flds. We have previously reported (26) a pH-dependent rate-limiting step for WT Fld reduction by the dRf radical, which was assigned to Fld semiquinone protonation. The putative protonation rate constant of Fld semiquinone (k_{prot}) after reduction by dRf has thus been determined with all mutants herein described, but no significant differences are observed between mutants and WT Fld (Table IV). From these findings we can infer that the ET rate constant determined at saturating Fld concentration (k_{et}) and the proposed protonation rate constant (k_{prot}) correspond to two unrelated, independent processes. Thus, our data indicate that whereas none of the replacements performed at position 94 or 57 promotes significant changes in the K_a value of the PSI_{rd}·Fld_{ox} complex under our standard conditions, some of the mutations promote drastic changes in the k_{et} from PSI to Fld. Remarkably, the k_{et} of Y94A Fld is 1 order of magnitude higher than that of WT, whereas replacement of Tyr^{94} by a tryptophan produces a virtually nonreactive protein (Table IV). Replacement of Tyr^{94} by phenylalanine has little effect on the reactivity of the flavoprotein, as compared with the other mutants at position 94, as expected for this conservative change. With regard to position 57, replacement of tryptophan with any smaller hydrophobic residue improves the ET from PSI to Fld. This effect is particularly relevant in W57F, whose k_{et} is 6 times higher than WT. The unexpected result is that replacement of tryptophan by tyrosine promotes the reverse effect, the ET rate constant decreasing 5 times relative to WT.

DISCUSSION

Trp^{57} and Tyr^{94}, which sandwich the isoalloxazine ring in *Anabaena* sp. PCC 7119 Fld, have been shown to influence its reduction potentials and absorption spectra and to strengthen the FMN apoflavodoxin interaction (11). In the present study, we have analyzed their influence on the Fld interaction and ET by measuring the functionality of different Fld mutants at positions 57 and 94 with its two physiological redox partners, FNR and PSI.

Steady-state and fast kinetic studies have been carried out to analyze the reactions of Fld with FNR. The K_m values obtained for FNR, using the different Fld variants as protein carriers in

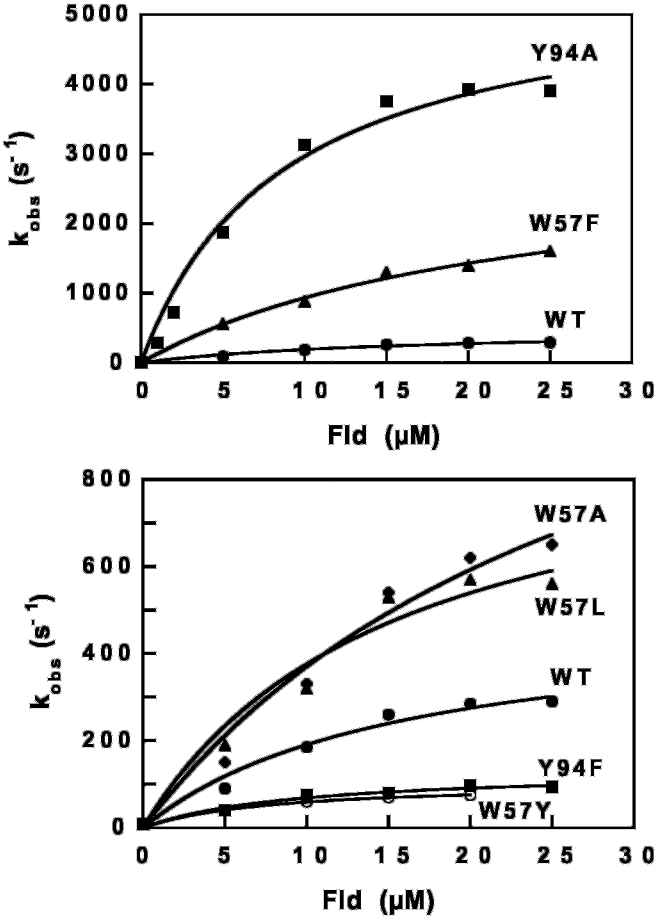

FIG. 5. **Dependence upon Fld concentration of the k_{obs} for reduction of WT and mutated Fld forms by *Anabaena* PSI.** Experimental conditions were as described under "Experimental Procedures." The *solid lines* have been obtained by fitting the experimental points to the formalism devised by Meyer *et al.* (25).

TABLE IV
Kinetic parameters for the reduction of WT and mutated Flds by Anabaena PSI and by deazariboflavin as studied by laser flash photolysis

Fld	Reduction by PSI		Reduction by dRf (k_{prot})[a]
	K_a	k_{et}	
	M^{-1}	s^{-1}	s^{-1}
WT	6.0×10^5	500	450
Y94A	7.0×10^5	5500	730
Y94F	8.0×10^5	135	610
Y94W	ND[b]	<100	410
W57F	3.0×10^5	2950	625
W57L	1.0×10^5	950	440
W57A	6.0×10^5	1480	580
W57Y	4.0×10^5	105	505

[a] The rate constants were estimated from the Fld concentration-independent kinetic traces followed at both 465 and 580 nm (see "Experimental Procedures").
[b] Not determined, due to extremely slow kinetics.

the NADPH-dependent cytochrome *c* reductase assay (Table I), as well as the data derived from differential spectroscopic analysis of the FNR_{ox}-Fld_{ox} interaction (Fig. 1, Table II) indicate that the introduced mutations do not produce any major effect in the stability of the FNR_{ox}·Fld_{ox} complex or in the functionality of the FNR_{rd}·Fld_{ox} complex. However, some of the mutations clearly alter the ET between the two proteins. The most noticeable alteration is produced upon replacement of Tyr^{94} by alanine. In this mutant, processes involving ET from FNR_{rd} to Fld_{ox} show rates up to 5-fold higher than those obtained with WT Fld when monitoring the FNR cytochrome *c* reductase activity (Table I) and up to 222-fold higher when following the direct reaction by stopped flow (Fig. 3*B*, Table III). Previous studies, however, had shown that FNR_{rd} is apparently not so well suited for transferring a single electron to WT Fld_{ox} as it is to Fd_{ox} ($E_m = -384$ mV) (29), whereas FNR_{sq} is much more efficient (rate constant $>7000\ s^{-1}$ (30)). These findings reveal the importance of the structural features of the proteins participating in ET processes over thermodynamic factors (18). Since, in the case of the Y94A mutant, the introduced side chain does not provide an electronic environment that can improve by itself the ET process, structural and thermodynamic aspects have to account for the enhancement observed. The reported reduction potentials for this mutant show an E_1 value considerably less negative than that for WT Fld (-299 mV *versus* -436 mV), indicating that in this mutant the entrance of the second electron is thermodynamically favored, which might allow a full reduction of Y94A Fld_{sq} by FNR_{rd} or even by FNR_{sq}. This could explain the high k_{cat} value observed for FNR in the NADPH-dependent cytochrome *c* reductase assay when using Y94A; once enough Y94A Fld_{rd} is formed, it might cycle between the hydroquinone and semiquinone states when transferring electrons from FNR to cytochrome *c*, thus working under a thermodynamic force closer to that operating in the Fd assay. However, an enhancement of the ET from FNR_{rd} to Fld_{ox} should not be discarded. To clarify this, we have followed the FNR_{rd}/Fld_{ox} reaction by stopped flow. The increase in absorbance observed at 600 nm (Fig. 3*B*) indicates a very fast accumulation of semiquinone states, which is not consistent with a two-electron transfer process and suggests a single electron transfer and accumulation of the two semiquinone species. Therefore, the larger efficiency observed when analyzing the ET from FNR_{rd} to Y94A Fld_{ox} has to be due to a faster single ET process to generate Y94A Fld_{sq}. Since complex formation is apparently not affected and the E_2 value for this mutant is similar to that for WT Fld, structural aspects have to account for the enhancement of the process. We suggest that replacement of the large tyrosine residue by the small alanine might help by simply making the flavin cofactor more accessible to reduction. Consistently, replacement of tyrosine by tryptophan (with a larger side chain) in the Y94W mutant would make the flavin cofactor less accessible, thereby explaining the lower ET rate from FNR_{rd} to the mutant, as shown by both steady-state and fast kinetic studies (Tables I and III). This hypothesis is supported by the structures reported for two mutants from *D. vulgaris* Fld, Y98H and Y98W, at a position equivalent to that of Tyr^{94} in *Anabaena* Fld (15). These structures show that, although the overall folding remains the same as that of native Fld, the environment of the isoalloxazine ring is modified by the introduced mutations. Noticeably, in both mutants the 60–64 loop, (Trp^{60} corresponds to Trp^{57} in the *Anabaena* Fld) is displaced and resembles more the structure of the Fld semireduced state than that of the oxidized state. Moreover, the hydrogen-bonding network and the water scheme around the FMN are different, and both mutant structures show a slight bending in the FMN isoalloxazine ring. In particular, the structure of the Y98W mutant clearly shows a larger shielding of the flavin from the solvent, especially at positions N-5, where a proton has to enter in order to produce the reduced and semiquinone states of FMN, and C-6 of the flavin ring. This strongly suggests that the observed decreased reactivity of Y94W *Anabaena* Fld in the ET processes with FNR is due to a decreased accessibility of the flavin cofactor. On the other hand, the structure of the Y98H mutant from *D. vulgaris* Fld shows less shielding of the flavin ring from the solvent, with the benzene ring fully exposed. This lack of shielding has been related with the noticeable E_1 shift to more positive values exhibited by this mutant (15). A similar E_1 shift has been found in our Y94A mutant (11), suggesting also a large accessibility of the isoalloxazine ring in this mutant, as expected for a Tyr to Ala replacement.

However, when analyzing the opposite process, reduction of FNR by Fld variants, Y94A ET is hindered relative to WT Fld. This is so because the introduced mutation produces an important alteration of the flavin E_1 value, which is 137 mV more positive than that of WT, making reduction of FNR ($E_m = -323$ mV (29)) much less favorable from the thermodynamic point of view. The Y94W, W57F, and W57Y Fld mutants (Fig. 2*B*) do not show any major alterations of the reduction potentials, yet they display a lag phase and slower and diminished processes. In these mutants, structural aspects must account for the observed lag phase, indicative of the accumulation of an intermediate prior to ET, and suggesting that complex reorganization cannot achieve the optimal orientation in the transition state for efficient ET.

Interaction and ET between reduced PSI and the different Flds were analyzed by using laser flash photolysis. For WT Fld, the obtained kinetic parameters are of the same order of magnitude as those previously described for the interaction of this flavoprotein with PSI from different sources (16, 28). The similar association constants obtained with either WT Fld or the different mutants for the PSI_{rd}·Fld_{ox} complex suggest that the binding ability of Fld to PSI is not affected by the introduced mutations (Table IV). As observed when analyzing reduction by FNR_{rd}, reduction of Y94A Fld by PSI presents a value of k_{et} much higher than WT. This must, again, be due to a higher accessibility of the flavin cofactor to reduction in the Y94A mutant. Consistent with this interpretation, Y94W is virtually nonreactive with PSI (Table IV). It is noticeable that whereas most replacements of Trp^{57} with smaller hydrophobic residues optimize the electron transfer from PSI to Fld with respect to WT, an important decrease is observed for the W57Y variant (Table IV). This finding clearly indicates that the hydroxyl group is impairing the ET reaction.

The aforementioned studies indicate that removal of the aromatic side chain in the Y94A mutant increases the accessibility of the cofactor to the FMN one-electron reduction process (Tables I, III, and IV), whereas thermodynamic factors would favor the entrance of the second electron (11), which would produce accumulation of Fld_{rd} in the cells upon light irradiation. However, the thermodynamic driving force would oppose ET from fully reduced Fld to its physiological substrate, FNR. Thus, our data clearly indicate that Tyr^{94} is not required for ET from PSI to FNR via Fld; however, the occurrence in Fld of a tyrosine residue at that position is necessary to modulate the FMN E_1 value and for a strong FMN binding (11). Moreover, it provides a compromise between efficient PSI/Fld and Fld/FNR ET. Previous studies suggested a possible role for Trp^{57} in the kinetics of Fld redox reactions (11). However, our data indicate that mutants at this position can accept electrons from FNR_{rd} as efficiently as WT (Table I and III) and much more efficiently from PSI (Table IV). Moreover, replacement of Trp^{57} by leucine

or alanine does not produce major alterations in the Fld ability to reduce FNR, although almost no reduction of W57F or W57Y Flds is detected. Our data, thus, indicate that Trp^{57} cannot be directly involved in the ET process itself but rather provides an appropriate structural and electronic environment while cooperating with Tyr^{94} in FMN binding (11).

In summary, in the ET process from PSI to FNR via Fld, the aromatic residues stacking the FMN cofactor appear not to be directly involved in the ET pathway. Thus, in the case of *Anabaena* Fld, the flavin environment, provided by Trp^{57} and Tyr^{94}, might not be the most "productive" one for each individual process, but it represents an efficient compromise for the different ET steps and allows a tight FMN binding in order to optimize the overall process of ET from PSI to $NADP^+$.

REFERENCES

1. Mayhew, S. G., and Tollin, G. (1992) in *Chemistry and Biochemistry of Flavoenzymes*, Vol. III (Müller, F., ed) pp. 389–426, CRC Press, Inc., Boca Raton, FL
2. Rogers, L. J. (1987) in *The Cyanobacteria* (Fay, P., and Van Baalen, C., eds) pp. 35–67, Elsevier Science Publishing Co., Inc., New York
3. Ludwig, M. L, and Luschinsky, C. L. (1992) in *Chemistry and Biochemistry of Flavoenzymes*, Vol. III (Müller, F., ed) pp. 427–466, CRC Press, Inc., Boca Raton, FL
4. Watenpaugh, K. D., Sieker, L. C., and Jensen, L. H. (1973) *Proc. Natl. Acad. Sci. U. S. A.* **70,** 3857–3860
5. Burnett, R. M., Darling, G. D., Kendall, D. S., Lequesne, M. E., Mayhew, S. G., Smith, W. W., and Ludwig, M. L. (1974) *J. Biol. Chem.* **249,** 4383–4392
6. Smith, W. W., Pattridge, K. A., Ludwig, M. L., Petsko, G. A., Tsernoglou, D., Tanaka, M., and Yasunobu, K. T. (1983) *J. Mol. Biol.* **165,** 737–753
7. Fukuyama, K., Wakabayashi, S., Matsubara, H., and Rogers, L. J. (1990) *J. Biol. Chem.* **265,** 15804–15812
8. van Mierlo, C. P. M., Lijnzaad, P., Vervoort, J., Müller, F., Verendsen, H. J., and de Vlieg, J. (1990) *Eur. J. Biochem.* **194,** 185–198
9. Rao, S. T., Shaffie, F., Yu, C., Satyshur, K. A., Stockman, B. J., Markley, J. L., and Sundaralingan, M. (1992) *Protein Sci.* **1,** 1413–1427
10. Genzor, C. G., Perales-Alcón, A., Sancho, J., and Romero, A. (1996) *Nat. Struct. Biol.* **3,** 329–332
11. Lostao, A., Gómez-Moreno, C., Mayhew, S. G., and Sancho, J. (1997) *Biochemistry* **36,** 14334–14344
12. Swenson, R. P., and Krey, G. D. (1994) *Biochemistry* **33,** 8505–8514
13. Zhou, Z. M., and Swenson, R. P. (1996) *Biochemistry* **35,** 15980–15988
14. Medina, M., Lostao, A., Sancho, J., Gómez-Moreno, C., Cammack, R., Alonso, P. J., and Martínez, J. (1999) *Biophys. J.* **77,** 1712–1720
15. Reynolds, R. A., Watt, W., and Watenpaugh, K. D. (2001) *Acta Crystallogr. Sec. D* **57**, 527–535
16. Navarro, J. A., Hervás, M., Genzor, C. G., Cheddar, G., Fillat, M. F., De la Rosa, M. A., Gómez-Moreno, C., Cheng, H., Xia, B., Chae, Y. K., Yan, H., Wong, B., Straus, N. A., Markley, J. L., Hurley J. K., and Tollin, G. (1995) *Arch. Biochem. Biophys.* **321,** 229–238
17. Jenkins, C. M., Genzor, C. G., Fillat, M. F., Waterman, M. R., and Gómez-Moreno, M. (1997) *J. Biol. Chem.* **36,** 22509–22513
18. Medina, M., Martínez-Júlvez, M., Hurley, J. K., Tollin, G., and Gómez-Moreno, C. (1998) *Biochemistry* **37,** 2715–2728
19. Rögner, M., Nixon, P. J., and Dinner, B. A. (1990) *J. Biol. Chem.* **265,** 6189–6196
20. Hervás, M., Ortega, J. M., Navarro, J. A., De la Rosa, M. A., and Bottin, H. (1994) *Biochim. Biophys. Acta* **1184,** 235–241
21. Mathis, P., and Sétif, P. (1981) *Isr. J. Chem.* **21,** 316–320
22. Arnon, D. I. (1949) *Plant Physiol.* **24,** 1–15
23. Shin, M. (1971) *Methods Enzymol.* **23,** 440–442
24. Hervás, M., Navarro, J. A., Díaz, A., Bottin, H., and De la Rosa, M. A. (1995) *Biochemistry* **34**, 11321–11326
25. Meyer, T. E., Zhao, Z. G., Cusanovich, M. A., and Tollin, G. (1993) *Biochemistry* **32,** 4552–4559
26. Navarro, J. A., Hervás, M., Pueyo, J. J., Medina, M., Gómez-Moreno, C., De la Rosa, M. A., and Tollin, G. (1994) *Photochem. Photobiol.* **60,** 231–236
27. Medina, M., Hervás, M., Navarro, J. A., De la Rosa, M. A., Gómez-Moreno, C., and Tollin, G. (1992) *FEBS Lett.* **313,** 239–242
28. Mühlenhoff, U., and Sétif, P. (1996) *Biochemistry* **35,** 1367–1374
29. Hurley, J. K., Weber-Main, A. N., Stankovich, M. T., Benning, M. M., Thoden, J. B., Vanhooke, J. L., Holden, H. M., Chae, J. K., Xia, B., Cheng, H., Markley, J. L., Martínez-Júlvez, M., Gómez-Moreno, C., Schmeits, J. L., and Tollin, G. (1997) *Biochemistry* **36,** 11100–11117
30. Walker, M. C., Pueyo, J. J., Gómez-Moreno, C., and Tollin, G. (1990) *Arch. Biochem. Biophys.* **281,** 76–83